PARAMETRIC INSTABILITY OF CROSS-PLY LAMINATED COMPOSITE CYLINDRICAL SHELLS BASED ON LARGE DEFLECTIONS THEORY

Darabi, Mehdi [1*], Ganesan, Rajamohan [1]
[1] Concordia Centre for Composites, Department of Mechanical and Industrial Engineering, Concordia University, Montreal, Canada
* m_darab@encs.concordia.ca

Keywords: *Dynamic Instability; Composite Laminates; Large Deflections; Cylindrical Shells.*

ABSTRACT

The parametric instability of thin simply supported laminated composite cylindrical shells under harmonically-varying in-plane loads is investigated. Dynamic instability analysis based on classical linear theories provided only an outline of the parameter regimes where nonlinear effects are of importance. Linear analysis carried out in available literature can only provide the information about the instability region and unable to predict the vibration amplitudes in these regions. In this work, to determine such vibration amplitudes as well as dynamically-unstable regions, Von-Karman-type of nonlinearity is taken into the account in the equations of motion. The procedure implemented in this work is based on using Airy's stress function and by combining the mid-plane strains, the nonlinear compatibility equation is derived. Consequently, by satisfying the two in-plane force-equilibrium equation, the general Galerkin method is used for the moment-equilibrium equation of motion according to the Donnell's shallow-shell theory to satisfy spatial dependence in the partial differential equation of motion to produce a set of non-linear Mathieu-Hill equations. These equations are ordinary differential equations, with time-dependency. By applying the Bolotin's method to these equations, the dynamically-unstable regions, stable-, and unstable-solutions amplitudes of the steady-state vibrations are obtained. Numerical results are also presented to bring out the influence of various parameters such as magnitude of both tensile and compressive axial loads, radius-to-thickness ratio and length-to-radius ratio as well, on the dynamic instability behavior of the studied laminated composite cylindrical shell.

1 INTRODUCTION

Shell structures are used in a multitude of thin-walled lightweight load bearing structural parts for various modern aerospace, offshore, nuclear, automative, and civil engineering structures. One of the main targets in the design of shell structural elements is to make the thickness as thin as possible to make the structure light. On the other hand composite structures are also increasingly being used in aerospace, mechanical and automative industries due to their high-strength-to-weight and stiffness-to-weight ratios. Acknowledging to the difficulty of analysis of shells related to the curvature the variation of material properties due to composite bring more complexity for the mechanical behavior of lamented composite shells. For their thin nature, they can present large deflections, with respect to the shell thickness, associated to small strains before collapse. Also shells are often subjected to dynamic loads that causes vibrations; vibration amplitude of the order of the shell thickness can be easily reached in many applications. Hence, for more perfect and complete studies of dynamic instability of laminated plates, the nonlinear analysis is required. When the lightweight structural components are subjected to dynamic loading particularly periodic in-plane loads, when the frequency of in-plane dynamic load and the frequency of vibration satisfy certain specific condition, parametric resonance will occur in the structure, which makes the shell to enter into a state of dynamic instability [1]. This instability is of concern because it can occur at load magnitudes that are much less than the static buckling load, so a component designed to withstand static buckling may fail in a periodic loading environment. Further, the dynamic instability occurs over a range of forcing frequencies rather than at a single value [1, 2]. A comprehensive study of the dynamic instability of the elastic systems, such as rods, plates and shells subjected to periodically varying loads has been given in the text by Bolotin [3]. The intensive use of fiber-reinforce composites has resulted lately in several studies of the dynamic instability of laminated shells and plates. Most of these works are based on linear analysis and so leads to only predicting the dynamic instability regions [4-8]. All these mentioned works are based on linear analysis and so lead to the determination of dynamic instability regions and unable to predict the vibration amplitudes in these regions.

In the present work, the instability regions as well as the both stable- and unstable- solutions amplitudes of steady-state vibrations are determined based on Donnell's nonlinear large deflection shell equations of motion which lead to a system of nonlinear Mathieu-Hill equations. The effect of magnitude of both tensile and compressive axial periodic loadings, aspect ratios i.e. radius-to-thickness ratio and length-to-radius ratio as well, on the dynamically-unstable regions and the amplitudes of the steady-state vibrations are investigated.

2 FORMULATION OF THE PROBLEM AND SOLUTION

A thin simply supported laminated composite cylindrical shell, having length L and radius R with respect to the curvilinear coordinates (X, θ, Z)which are assigned in the mid-surface of the shell is considered as shown in Fig.1. Here, u, v and w are the displacement components of the shell with reference to this coordinate system in the X, θ, Z, directions, respectively.

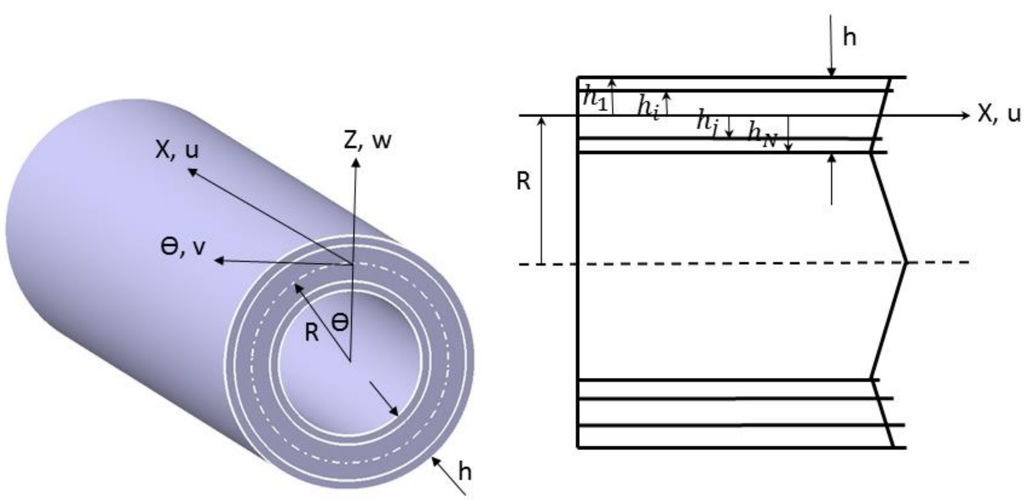

Figure 1. The geometry of a laminated composite cylindrical shell and the cross-sectional view.

The cylindrical shell is subjected to a periodically pulsating load in the axial direction with the axial loading per unit length as follow:

$$F_{xx}(t) = F_s + F_d cosPt \tag{1}$$

where F_s is a time invariant component, $F_d cosPt$ is the harmonically pulsating component, and P denotes the frequency of excitation in radians per unit time.

Since $u_0 \ll w_0$ and $v_0 \ll w_0$ we can consider that $\rho_t \, {\partial^2 u_0}/{\partial t^2} \to 0$ and $\rho_t \, {\partial^2 v_0}/{\partial t^2} \to 0$. Therefore the equations of motion based on Donnell's theory under the axial pulsating load are given by

$$\frac{\partial N_{xx}}{\partial x} + \frac{1}{R}\frac{\partial N_{x\theta}}{\partial x} = 0 \tag{2}$$

$$\frac{\partial N_{x\theta}}{\partial x} + \frac{1}{R}\frac{\partial N_{\theta\theta}}{\partial \theta} = 0 \tag{3}$$

$$\frac{\partial^2 M_{xx}}{\partial x^2} + \frac{2}{R}\frac{\partial^2 M_{x\theta}}{\partial x \partial \theta} + \frac{1}{R^2}\frac{\partial^2 M_{\theta\theta}}{\partial \theta^2} - \frac{1}{R} N_{\theta\theta} + N_{xx}\frac{\partial^2 w_0}{\partial x^2} = \rho_t \frac{\partial^2 w_0}{\partial t^2} \tag{4}$$

where

$$\rho_t = \int_{-h/2}^{h/2} \rho \, dz, \tag{5}$$

and $(N_{xx}, N_{\theta\theta}, N_{x\theta})$ are the total in-plane force resultants and $(M_{xx}, M_{\theta\theta}, M_{x\theta})$ are the total moment resultants . The nonzero von Karman strains associated with nonlinear large deflections and curvatures are given by

$$\begin{Bmatrix} \epsilon_{xx} \\ \epsilon_{yy} \\ \gamma_{xy} \end{Bmatrix} = \begin{Bmatrix} \frac{\partial u_0}{\partial x} + \frac{1}{2}(\frac{\partial w_0}{\partial x})^2 \\ \frac{1}{R}(\frac{\partial v_0}{\partial \theta} + w_0) + \frac{1}{2R^2}(\frac{\partial w_0}{\partial \theta})^2 \\ \frac{1}{R}\frac{\partial u_0}{\partial \theta} + \frac{\partial v_0}{\partial x} + \frac{1}{R}\frac{\partial w_0}{\partial x}\frac{\partial w_0}{\partial \theta} \end{Bmatrix} + \mathrm{z} \begin{Bmatrix} -\frac{\partial^2 w_0}{\partial x^2} \\ -\frac{1}{R^2}\frac{\partial^2 w_0}{\partial \theta^2} \\ -\frac{2}{R}\frac{\partial^2 w_0}{\partial x \partial \theta} \end{Bmatrix} \tag{6}$$

The force and moment resultants are defined in terms of A_{ij} extensional stiffnesses A_{ij}, the bending stiffnesses D_{ij}, the bending-extensional coupling stiffnesses B_{ij}, membrane strains and the flexural (bending) strains as well. Then we define the membrane forces in terms of Airy's stress function φ as

$$N_{xx} = \frac{1}{R^3}\frac{\partial^2 \phi}{\partial \theta^2} \tag{7a}$$

$$N_{\theta\theta} = \frac{\partial^2 \phi}{\partial x^2} \tag{7b}$$

$$N_{x\theta} = -\frac{1}{R}\frac{\partial^2 \phi}{\partial x \partial \theta} \tag{7c}$$

Hence, the strains and moment resultants are obtained in terms of the Airy's stress function ϕ and w_0. By combining the mid-plane strains, the compatibility equation can be expressed as

$$\frac{\partial^2 \epsilon_{\theta\theta}^{(0)}}{\partial x^2} + \frac{1}{R^2}\frac{\partial^2 \epsilon_{xx}^{(0)}}{\partial \theta^2} - \frac{1}{R}\frac{\partial^2 \gamma_{x\theta}^{(0)}}{\partial x \partial \theta} = \frac{1}{R}\frac{\partial^2 w}{\partial x^2}\frac{\partial^2 w_0}{\partial \theta^2} + \frac{1}{R^2}\frac{\partial^2 w_0}{\partial x \partial \theta} \tag{8}$$

Then replacing the strains in terms of the Airy's stress function ϕ and w_0 the non-linear equation of compatibility is derived. Considering the simply supported boundary condition the transverse displacement function $w_0(x, y, t)$ is chosen as

$$w_0 = \sum_{m=1}^{\infty}\sum_{n=1}^{\infty} q_{mn}(t) \sin\frac{m\pi}{L}x \cos n\theta \tag{9}$$

where m and n represent the number of longitudinal and transverse half waves in corresponding standing wave pattern, respectively. The first two equations of motion (2) and (3) are satisfied automatically only by replacing (7a-7c). Solving Airy's stress function ϕ in terms of $q_{mn}(t)$ considering the axial loads applied at the edge, and then substituting in the forces and moments resultants, bring all them in the third equation of motion (4) and after multiplying the governing equation by $\sin\frac{m\pi}{L}x \cos n\theta$ and integrating over the plate area, a system of $m \times n$ second-order ordinary differential equations is obtained:

$$M_{mn}\ddot{q}_{mn}(t) + K_{mn}q_{mn}(t) - (F_s + F_d\cos pt)Q_{mn}q_{mn}(t) + \eta_{mn}q_{mn}^3(t) = 0 \tag{10}$$

where M_{mn}, K_{mn}, Q_{mn} and η_{mn} are matrices in terms of extensional, bending, bending-extensional coupling stiffnesses, shell's geometry properties and wave numbers for the studied laminate composite cylindrical shell. Introducing following notation:

$$\omega_{mn} = \sqrt{\frac{K_{mn}}{M_{mn}}} \tag{11}$$

$$\gamma_{mn} = \frac{\eta_{mn}}{M_{mn}} \tag{12}$$

$$N_* = \frac{K_{mn}}{Q_{mn}} \tag{13}$$

Equation (12) can be written in the form of the nonlinear Mathieu equation as follow:

$$\ddot{q}_{mn}(t) + \Omega_{mn}^2(1 - 2\mu_{mn}\cos pt)q_{mn}(t) + \gamma_{mn}q_{mn}^3(t) = 0 \tag{14}$$

where

$$\Omega_{mn} = \omega_{mn}\sqrt{1 - \frac{F_s}{N_*}} \tag{15}$$

$$\mu_{mn} = \frac{F_d}{2(N_* - F_s)} \tag{16}$$

Using Bolotin's [3] method for parametric vibration, the solution of period $2T$ considering the first approximation is given by the following equation:

$$q(t) = a\sin\frac{Pt}{2} + b\cos\frac{Pt}{2} \tag{17}$$

By substitution of (17) into (14) a system of two homogeneous linear equations with respect to a and b can be obtained. This system has solutions that differ from zero only in the case where the determinant composed of the coefficients is equal to zero:

$$\begin{vmatrix} 1 + \mu_{mn} - n_{mn}^2 + \frac{3\gamma_{mn}}{4\Omega_{mn}^2}A^2 & 0 \\ 0 & 1 - \mu_{mn} - n_{mn}^2 + \frac{3\gamma_{mn}}{4\Omega_{mn}^2}A^2 \end{vmatrix} = 0 \tag{18}$$

where A is the amplitude of steady-state vibrations and is given by:

$$A = \sqrt{a^2 + b^2} \tag{19}$$

and

$$n_{mn} = \frac{P}{2\Omega_{mn}} \tag{20}$$

Expanding the determinant and solving the resulting equation with respect to the amplitude, A, two solutions are obtained for A which are called stable-solution and unstable-solution corresponding to $+\mu_{mn}$ and $-\mu_{mn}$ respectively.

Also the dynamically unstable regions are determined by either linear part of Mathieu-Hill equation (14) or setting $A = 0$ in (18) and solving for excitation frequency P in the more simplified form of an eigenvalue problem as follow:

$$\begin{vmatrix} K_{mn}^* - \frac{Q_{mn}^*}{2} & 0 \\ 0 & K_{mn}^* + \frac{Q_{mn}^*}{2} \end{vmatrix} - P^2 \begin{vmatrix} \frac{M_{mn}}{4} & 0 \\ 0 & \frac{M_{mn}}{4} \end{vmatrix} = 0 \tag{21}$$

where

$$K_{mn}^* = K_{mn} - F_sQ_{mn} \tag{22}$$

$$Q_{mn}^* = F_d Q_{mn} \tag{23}$$

3 RESULTS AND DISCUSSIONS

The material properties used in the present analysis are chosen in accordance with Ng et al. [5] as $E_1/E_2 = 40$, $G_{12}/E_2 = 0.5$ and $\upsilon_{12} = 0.25$.
Figure 2 displays the boundaries of the first (from left to the right of the frequency axis) dynamically-unstable region (Fig. 2a) and both the stable- and unstable-solution amplitude of steady-state vibrations (Fig. 2b) of a two-layered antisymmetric $(90^{\circ}, 0^{\circ})$ cross-ply laminated cylindrical shell having thickness ratio of $L/R = 2$ and $R/h = 200$ subjected to tensile loading of $F_s = 0.1N_{cr}$.where N_{cr} is the critical buckling load which is approximated as [8]

$$N_{cr} = \frac{E_2 h^2}{R\sqrt{[3(1-\nu_{12}\nu_{21})]}} \tag{24}$$

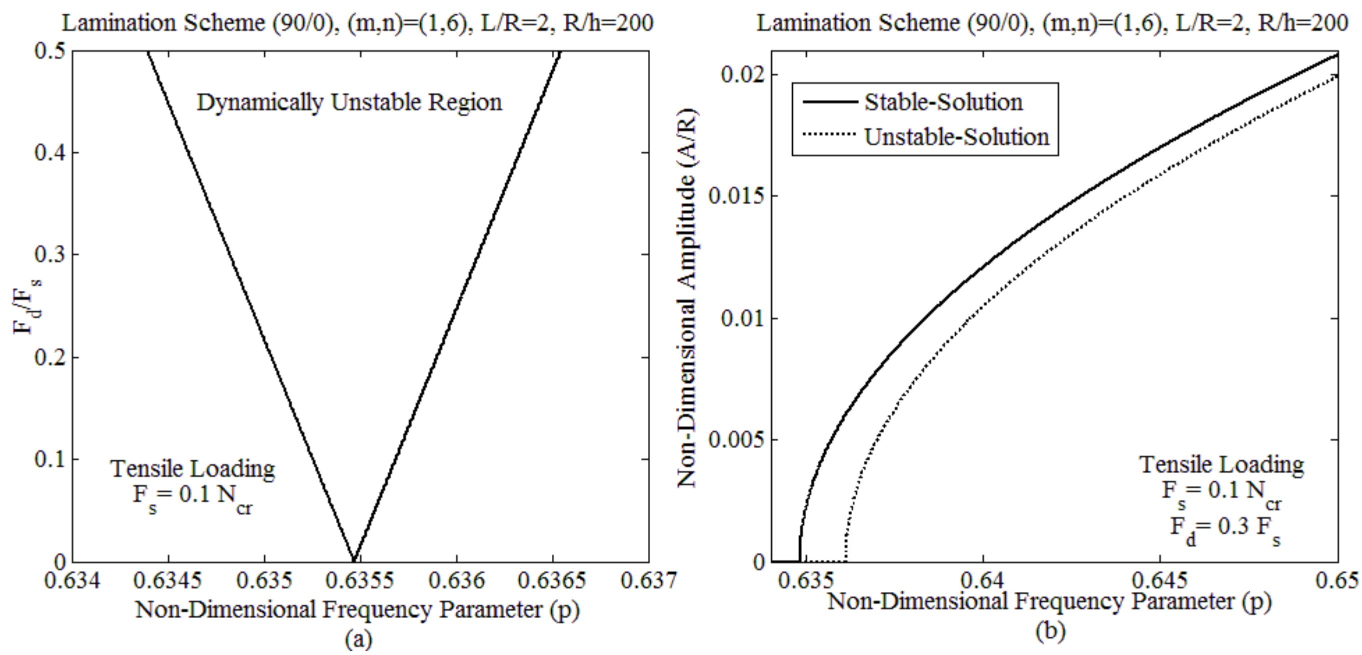

Figure 2. First mode a) unstable region and b) stable- and unstable-solution amplitude of steady-state vibrations of two- layered $(90^o/0^o)$ cross-ply laminated cylindrical shell having aspect ratios of $L/R = 2$ and $R/h = 200$ subjected to tensile loading of $F_s = 0.1N_{cr}$.

This approximates the static buckling load for laminated cylindrical shell and hence for the dynamic instability analysis both the static part of the load F_s and the periodic part F_d in Eq. (1) should be a percentage of this buckling load. As it can be observed from this figure each unstable region is separated by two lines with a common point of origin. Actually these two lines are not completely straight and they curved slightly outward. To compare the results in the following tables we specified each unstable regions by the non-dimensional frequency parameter p as $p = 2\pi RP\sqrt{\frac{\rho_t}{A_{11}}}$ of the point of origins and the half angle of the unstable regions as θ. In the analysis of dynamic stability of shells, there exists simultaneously the stable and unstable solutions. It is a characteristic of the nonlinear response that the resonance curves are bent toward the axis of increasing frequencies [3]. The difference between these two solutions refers to the required magnitudes of frequency and amplitude to stimulate a parametric resonance. If this difference between them is small, then there might be the possibility of occurring parametric resonance. If the difference is large, it means high values of vibration frequency and amplitude are needed to stimulate a possible parametric resonance. The dynamic stability of such a plate or shell system is said to be good [1]. The zero stable- and unstable-solution amplitudes of this figure exactly coincide with the left and right curves of corresponding unstable regions, respectively shown in Figure 2a and the range of frequencies between these two solutions at $A = 0$ predicate the dynamically-unstable regions at this certain value of dynamic load factor F_d/F_s. So this figure shows graphically that unstable regions could be obtained by setting $A = 0$ in equation (18) and it could be considered as a validation of this nonlinear part of dynamic instability analysis.

The effects of variation of the magnitude of the tensile and compressive axial harmonically pulsating load on the dynamically-unstable regions and both the stable-and unstable-solution amplitudes of the steady-state vibrations, the results are presented in the Tables 1 and 2, respectively.

Load			1st Mode $(m,n) = (1,6)$	2nd Mode $(m,n) = (1,5)$
$F_s = 0.1N_{cr}$	Point of origin p $(\times 10^{-1})$	Present	6.3547085	6.3959595
		Ref. [6]	5.6544179	5.9596621
	θ $(\times 10^{-3})$	Present	2.1550190	2.1411435
		Ref. [6]	2.4095530	2.2971360
$F_s = 0.2N_{cr}$	Point of origin p $(\times 10^{-1})$	Present	6.3977001	6.4386756
		Ref. [6]	5.7026828	6.0054732
	θ $(\times 10^{-3})$	Present	4.2775352	4.2504033
		Ref. [6]	4.7959232	4.5549685
$F_s = 0.3N_{cr}$	Point of origin p $(\times 10^{-1})$	Present	6.4404047	6.4811102
		Ref. [6]	5.7505425	6.0509375
	θ $(\times 10^{-3})$	Present	6.3686202	6.3288172
		Ref. [6]	7.1268993	6.7749563
$F_s = -0.1N_{cr}$	Point of origin p $(\times 10^{-1})$	Present	6.2678408	6.3096597
		Ref. [6]	5.5566307	5.8669669
	θ $(\times 10^{-3})$	Present	2.1886489	2.1741179
		Ref. [6]	2.4634550	2.3333558
$F_s = -0.2N_{cr}$	Point of origin p $(\times 10^{-1})$	Present	6.2239523	6.2660642
		Ref. [6]	5.5070860	5.8200656
	θ $(\times 10^{-3})$	Present	4.4121140	4.3823579
		Ref. [6]	4.9655192	4.6995054
$F_s = -0.3N_{cr}$	Point of origin p $(\times 10^{-1})$	Present	6.1797521	6.2221631
		Ref. [6]	5.4570915	5.7727834
	θ $(\times 10^{-3})$	Present	6.6716455	6.6259279
		Ref. [6]	7.5075589	7.0994407

Table 1. The first two unstable regions of a two-layered $(90^{\circ}/0^{\circ})$ antisymmetric cross-ply laminated cylindrical shells having aspect ratios of $L/R = 2$ and $R/h = 200$ subjected to various tensile and compressive loading.

Comparing the results indicates that increasing the magnitude of tensile axial periodic loads results in increasing the corresponding excitation frequencies that causes instability, which means shifting dynamically-unstable regions to the right along the frequency axis (Table 1), and consequently decreasing the amplitude of steady-state vibrations (Table 2). The inverse trend can be seen in the case of compressive loading; increasing the magnitude of compressive longitudinal periodic loads results in decreasing the corresponding excitation frequencies that causes instability, which means shifting dynamically-unstable regions to the left along the frequency axis (Table 1), and consequently increasing amplitude of steady-state vibrations (Table 2). These outcomes can be expected because increasing the tensile axial load makes the shell to be stiffer, and contrarily increasing the compressive axial load results in decreasing the shell's stiffness. The results also illustrate that width of instability regions are increased once the absolute value of magnitude of in-plane loads are increased for both tensile and compressive loading conditions. All these outcomes are in an excellent conformance with those reported by Ng et al. [6] and also in terms of the accuracy of the results there are good agreements between these two studies.

Load	Non-Dimensional Amplitude (A/R)	1st Mode $(m,n)=(1,5)$	2nd Mode $(m,n)=(1,4)$
$F_s=0.1N_{cr}, F_d=0.3F_s$	Stable-Solutions $(\times 10^{-2})$	10.03062259	9.193301364
	Unstable-Solutions $(\times 10^{-2})$	10.0124106	9.173427196
$F_s=0.3N_{cr}, F_d=0.3F_s$	Stable-Solutions $(\times 10^{-2})$	9.926979564	9.080105931
	Unstable-Solutions $(\times 10^{-2})$	9.871669205	9.019603836
$F_s=0.5N_{cr}, F_d=0.3F_s$	Stable-Solutions $(\times 10^{-2})$	9.822242973	8.965481442
	Unstable-Solutions $(\times 10^{-2})$	9.72889201	8.863111204
$F_s=-0.1N_{cr}, F_d=0.3F_s$	Stable-Solutions $(\times 10^{-2})$	10.15120088	9.324713383
	Unstable-Solutions $(\times 10^{-2})$	10.1332056	9.305119893
$F_s=-0.3N_{cr}, F_d=0.3F_s$	Stable-Solutions $(\times 10^{-2})$	10.28811899	9.473583948
	Unstable-Solutions $(\times 10^{-2})$	10.23476048	9.415610573
$F_s=-0.5N_{cr}, F_d=0.3F_s$	Stable-Solutions $(\times 10^{-2})$	10.42323872	9.620151037
	Unstable-Solutions $(\times 10^{-2})$	10.33531752	9.524819615

Table 2. The stable- and unstable-solution amplitudes corresponding to first two modes of steady-state vibrations for a ten-layered $(90^{\circ},0^{\circ})_5$ antisymmetric cross-ply laminated cylindrical shell having aspect ratios of $L/R=2$ and $R/h=200$ to various tensile and compressive loading under the excitation with non-dimensional frequency parameter $p=1$.

The effects of variation of the length-to-radius ratio L/R on the stable-solution amplitude of steady-state vibrations are shown in Figure 3 for the eight-layered $(90^{\circ},0^{\circ})_4$ cross-ply laminated cylindrical shell having thickness ratio $R/h=100$ subjected to the axial tensile loading of $F_s=0.5N_{cr}$ and $F_d=0.3F_s$. As expected at the specific excitation frequency the shell having higher aspect ratio L/R has a larger amplitude or in other words the corresponding excitation frequency that causes instability shifts to the left of frequency axis corresponding to lower frequencies, once the aspect ratio L/R is increased. This is due to the fact that increasing the length of the shell makes the shell to be less stiff.

It is also observed from the Figure 3 that by increasing the length, the circumferential wave numbers corresponding to the first two modes approach successively to lower values. The first two modes at $L/R=1$ are modes $(1,5)$ and $(1,4)$, for $L/R=5$ they are modes $(1,4)$ and $(1,3)$, and for $L/R=10$ they are modes $(1,3)$ and $(1,2)$ respectively.

To examine the effect of the thickness ratio R/h on the stable-solution amplitude of steady-state vibrations for the eight-layered $(90^{\circ},0^{\circ})_4$ cross-ply laminated cylindrical shell with length ratio $L/R=2$ subjected to axial compressive loading of $F_s=-0.3N_{cr}$ and $F_d=0.3F_s$ the results are presented in Figure 4. Here the first two modes are modes $(1,5)$ and $(1,4)$ respectively. It shows that by increasing the thickness ratio R/h, at any specific frequency, the amplitude of steady-state vibrations is increased or in other words the corresponding frequency of excitation that causes instability shifts to the left of frequency axis having lower frequencies. This is again due to the fact that decreasing the thickness of the shell makes the shell to be less stiff.

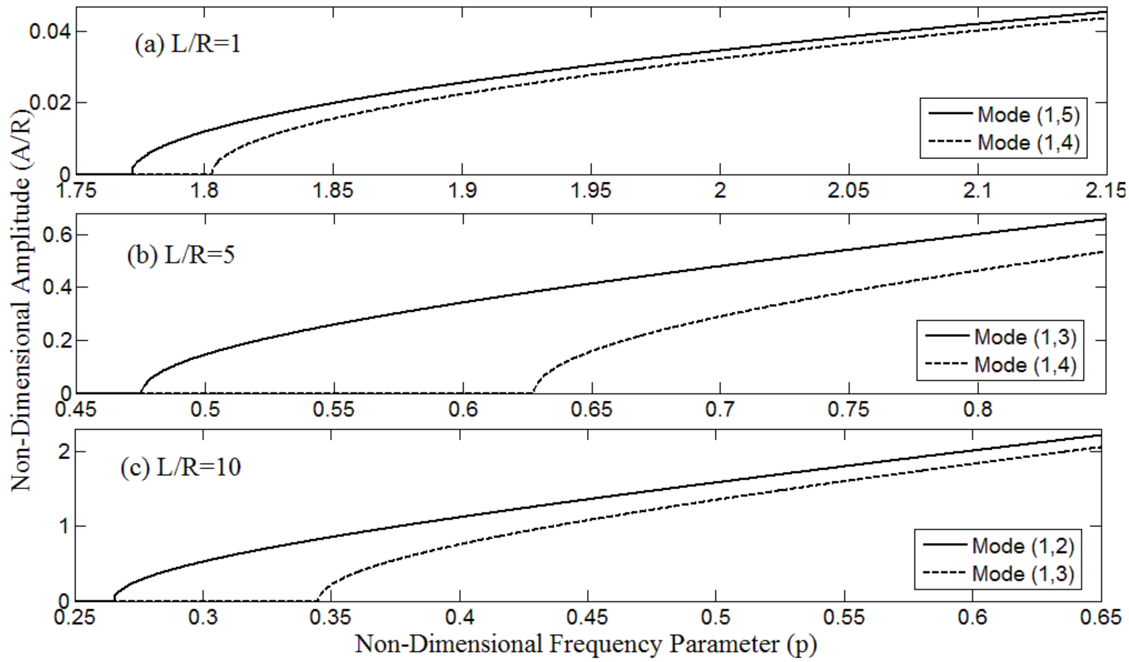

Figure 3. Variation of the first two stable-solution amplitudes of steady-state vibrations with shell length of an eight-layered $(90^{\circ}, 0^{\circ})_4$ antisymmetric cross-ply laminated cylindrical shell having thickness ratio $R/h = 100$ subjected to tensile loading of $F_s = 0.5N_{cr}$ and $F_d = 0.3F_s$

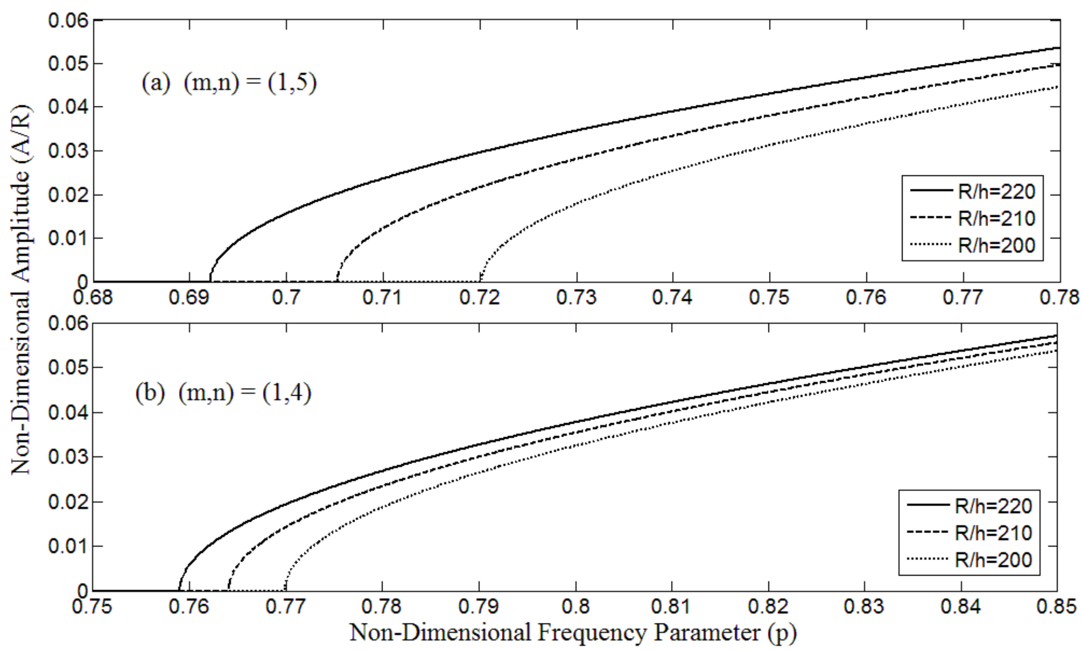

Figure 4. Variation of the first two stable-solution amplitudes of steady-state vibrations with shell thickness of an eight-layered $(90^{\circ}, 0^{\circ})_4$ antisymmetric cross-ply laminated cylindrical shell having length ratio $L/R = 2$ subjected to compressive loading of $F_s = -0.3N_{cr}$ and $F_d = 0.3F_s$

4 CONCLUSION

The non-linear dynamic stability of antisymmetric cross-ply laminated composite cylindrical shells under combined static and periodic axial loading has been studied. The results indicted that increasing the magnitude of tensile longitudinal periodic loads results in shifting dynamically-unstable regions to the right along the frequency axis, and consequently decreasing the amplitude of steady-state vibrations. However, increasing the magnitude of compressive longitudinal periodic loads causes shifting dynamically-unstable regions to the left along the frequency axis, and consequently increasing amplitude of steady-state vibrations. Albeit increasing either the magnitude of the tensile or compressive axial periodic loads results in increasing the widths of instability regions.

It is also concluded that increasing either length-to-radius L/R or radius-to-thickness R/h of the cylindrical shells makes the shell be less stiff consequently at any specific frequency, the amplitude of steady-state vibrations increased or in other words the corresponding frequency of excitation that causes instability shifts to the left of frequency axis having lower frequencies.

A comparative study of the present work with those available in literature shows a very good agreement. However, as the results of the present study reveal, the linear analysis carried out in available literature can only provide the information about the instability region and unable to predict the vibration amplitudes in these regions. The non-linear analysis developed in the present work can determine such vibration amplitudes.

5 ACKNOWLEDGEMENT

The authors thank the Faculty of Engineering and Computer Science at Concordia University, and Natural Sciences and Engineering Research Council of Canada (NSERC) for their financial support for the research work conducted. The NSERC support was provided through the Discovery Grant # 172848-2012 to the second author of the present paper.

6 REFERENCES

[1] Darabi, M.; Darvizeh, M.; Darvizeh, A.;, "Non-linear analysis of dynamic stability for functionally graded cylindrical shells under periodic axial loading," *Composite Structures,* vol. 83, pp. 201-211, 2008.

[2] Argento, A.; Scott, R. A.;, "Dynamic instability of layered anisotropic circular cylindrical shells, part I: Theoretical development," *Sound and vibrations,* vol. 162, no. 2, pp. 311-322, 1993.

[3] Bolotin, V. V.;, The dynamic stability of elastic systems, San Francisco: Holden-Day, 1964.

[4] A. Argento, "Dynamic instability of a composite circular cylindrical shell subjected to combined axial and torsional loading," *Composite Materials,* vol. 27, pp. 1722-1738, 1993.

[5] Ng, T. Y.; Lam, K. Y.; Reddy, J. N.;, "Dynamic stability of cross-ply laminated composite cylindrical shells," *Int. J. Mechanical Science,* vol. 40, no. 8, pp. 805-823, 1998.

[6] K. Y. Lam and T. Y. Ng, "Dynamic stability analysis of laminated composite cylindrical shells subjected to conservative periodic axial loads," *Composite Part B,* vol. 29B, pp. 769-785, 1998.

[7] Sahu, S. K.; Datta, P. K.;, "Research advances in the dynamic stability behavior of plates and shells: 1987–2005—part I: conservative systems," *Sahu, S. K., and P. K. Datta. "Research advances in the dynamic stability behavior of plateApplied mechanics reviews,* vol. 60, no. 2, pp. 65-75, 2007.

[8] Liew, K. M.; Hu, Y. G.; Zhao, X.; Ng., T. Y., "Dynamic stability analysis of composite laminated cylindrical shells via the mesh-free kp-Ritz method," *computer methods in applied mechanics and engineering,* vol. 196, pp. 147-160, 2006.

[9] Ovesy, H. R.; Fazilati, J.;, "Parametric instability analysis of laminated composite curved shells subjected to non-uniform in-plane load," *Composite Structures,* vol. 108, pp. 449-455, 2014.